

REPORT DOCUMENTATION PAGE

2

1a. REPORT SECURITY CLASSIFICATION  
Unclassified

DTIC

1b. RESTRICTIVE MARKINGS  
DTIC FILE COPY

2a. SECURITY CLASSIFICATION AUTHORITY

ELECTE

3. DISTRIBUTION / AVAILABILITY OF REPORT  
Approved for public release; distribution is unlimited.

NOV 16 1990

5. MONITORING ORGANIZATION REPORT NUMBER(S)  
AFOSR-TR- 90 1119

AD-A229 435

NUMBER(S)  
D

6b. OFFICE SYMBOL (if applicable)  
University of Washington

7a. NAME OF MONITORING ORGANIZATION  
AFOSR/NA

6c. ADDRESS (City, State, and ZIP Code)  
Department of Aeronautics and Astronautics  
University of Washington  
Seattle, WA 98195

7b. ADDRESS (City, State, and ZIP Code)  
Building 410, Bolling AFB DC  
20332-6448

8a. NAME OF FUNDING / SPONSORING ORGANIZATION  
AFOSR/NA

8b. OFFICE SYMBOL (if applicable)  
NA

9. PROCUREMENT INSTRUMENT IDENTIFICATION NUMBER  
AFOSR 87-0366

8c. ADDRESS (City, State, and ZIP Code)  
Building 410, Bolling AFB DC  
20332-6448

10. SOURCE OF FUNDING NUMBERS			
PROGRAM ELEMENT NO.	PROJECT NO.	TASK NO.	WORK UNIT ACCESSION NO.
61102F	2308	A2	

11. TITLE (Include Security Classification)  
(U)Turbulent Mixing in Exponential Transverse Jets

12. PERSONAL AUTHOR(S)  
Robert E. Breidenthal

13a. TYPE OF REPORT  
Final

13b. TIME COVERED  
FROM 8/01/88 TO 7/31/90

14. DATE OF REPORT (Year, Month, Day)  
9/31/90

15. PAGE COUNT

16. SUPPLEMENTARY NOTATION

17. COSATI CODES		
FIELD	GROUP	SUB-GROUP

18. SUBJECT TERMS (Continue on reverse if necessary and identify by block number)  
Transverse Jets, Turbulent Mixing, Accelerating Flows.

19. ABSTRACT (Continue on reverse if necessary and identify by block number)  
The effects of acceleration on vortex growth and molecular mixing have been systematically explored for the first time in a transverse array of exponentially increasing jets. The issue is the influence of a new kind of forcing which imposes on a vortex a time scale from an exponential rather than a sinusoidal wave. The results are that such forcing dramatically reduces the normalized size of the vortex. Therefore the capacity for mixed fluid inside the vortex is also reduced, by about a factor of eight at large acceleration.

20. DISTRIBUTION / AVAILABILITY OF ABSTRACT  
 UNCLASSIFIED/UNLIMITED  SAME AS RPT  DTIC USERS

21. ABSTRACT SECURITY CLASSIFICATION  
Unclassified

22a. NAME OF RESPONSIBLE INDIVIDUAL  
Julian M. Tishkoff

22b. TELEPHONE (Include Area Code)  
(202)767-0465

22c. OFFICE SYMBOL  
AFOSR/NA

(u)

## INTRODUCTION

While there has been extensive research on the response of vortices in free shear flows to sinusoidal forcing (Oster and Wagnanski, 1982), evidently the other most natural function had never been tested. The exponential function is an obvious choice. It is the only nontrivial function equal to its own derivative. Phenomenological and intuitive notions suggested that such a function might induce unusual behavior in turbulent vortices, Breidenthal (1986). An exponential array of transverse jets was chosen to test the hypothesis.

In compressible flow, such an array has another interesting feature. Shock losses are much less than in a conventional single transverse jet. Experiments with arrays at Mach three here by Clement and Rodriguez (1989) and Weiser (1990) reveal much weaker, more oblique shock systems than from a single round transverse jet. The supersonic primary flow is turned more gently by the array. This feature alone makes such arrays attractive in high speed propulsion applications.

## RESEARCH OBJECTIVES

The objective of this research is to test the hypothesis that exponential acceleration inhibits the mixing of momentum and mass. The size and penetration of the longitudinal vortex pair resulting from transverse injection were measured as a function of an acceleration parameter. The flame length of the jets is a direct measurement of the molecular scale mixing rate.

## ACCOMPLISHMENTS

From observations of the trajectory, and cross-sectional size of the vortices, as well as the flame length, our measurements reveal the following:

- i) Under acceleration, the roll up and growth of vortices is dramatically inhibited. For acceleration parameters of two or greater, the vortex cross sectional area is reduced by a factor of about eight from the nonaccelerating value.
- ii) Under increasing acceleration, the penetration of the transverse jet is as much as about 30% greater than that of a single nozzle, and the induced penetration occurs primarily in the far field, long after the acceleration is over.
- iii) The far field flame lengths are a weak maximum when the acceleration parameter  $\alpha$  is about unity. For large  $\alpha$ , flame lengths slowly decline with increasing  $\alpha$ , in remarkable contrast to the behavior of conventional jets.
- iv) A model for the exponential jet at large  $\alpha$  has been developed. It recognizes the dominant mixing role of the momentum defect in the wake component of the injected fluid.
- v) The size of the normal shock zone essentially depends only on the first nozzle in the array in a Mach three test. Therefore this dissipative region can be made as small as desired by using a sufficiently small first nozzle in an array.

The results suggest that an accelerating jet with oblique injectors, which mitigate or eliminate the longitudinal momentum defect, would permit a study of the far-field flow untainted by wake effects. In particular, for propulsion applications, it is important to

determine the speed with which the forced, near-field flow relaxes back to the unforced self-similar flow. If this transition is rapid, then the effect of acceleration on the inhibition of mixing would rapidly disappear in the far field, and the flame lengths would tend to coincide with those of the single transverse jet. In other words, the near-field mixing would be inhibited, but as soon as the forcing is over, the fluids would rapidly mix together.

On the other hand, if the transition is slow for some reason, the mixing rate would remain low for some time. In order to determine this transition, a spatial experiment with oblique jets or a temporal experiment is needed. An apparatus for the latter was constructed, but the experiments in it have not yet been completed. However, preliminary indications are that the jet spreading angle is dramatically reduced during acceleration.

### Compressibility Effects

In an independent project in our laboratory, two undergraduate students, Clement and Rodriguez, compared the shock wave structure from a conventional and an exponential transverse jet, both choked with the same thrust and mass flow. With orthogonal injection of helium, the jets generated shock waves in the primary flow, which was Mach three air. As expected, the conventional jet from a single orifice generated a bow shock which was normal near the nozzle, implying large losses in total pressure. However, the exponential array generated an essentially oblique shock, with much lower losses.

Ongoing tests by Weiser in the same supersonic tunnel but with a different nozzle array continue to explore the dependence of the shock structure on acceleration. The size of the normal shock zone depends only on the first nozzle size and thrust. The flow from the downstream nozzles is effectively shielded by that from the first nozzle. If the latter is small, then the extent of the highly dissipative, normal shock region is small.

### PUBLICATIONS

Clement, P. and Rodriguez, C. (1989) Shock wave structure and penetration height in transverse jets, winner of the national AIAA student paper contest, AIAA Student Journal, Vol. 27, No. 2, Summer 1989, pp. 7-16.

Eroglu, A. and Breidenthal, R. (1989) Penetration and mixing of accelerating jets in cross-flow, Amer. Phys. Soc./DFD meeting, NASA Ames, November 19-21, 1989.

Eroglu, A. (1990) Turbulent mixing in accelerating transverse jets, AIAA 21<sup>st</sup> Fluid Dynamics, Plasma Dynamics and Lasers Conference, June 18-20, 1990, Seattle, WA, AIAA Paper 90-1619.

Eroglu, A. (1991) Effects of exponential acceleration and pulsing on the mixing of a jet in a crossflow. Ph.D. Thesis University of Washington, in preparation.

### PERSONNEL

Professor R. Breidenthal	Principal Investigator	6%
Mr. A. Eroglu	Ph.D. Student	50%
Mrs. H. Li	M.S. Student	50%
Mr. L. Weiser	Visiting Scholar from France	



<input checked="" type="checkbox"/>
<input type="checkbox"/>
<input type="checkbox"/>
Codes
/ or
cial
A-1

## INTERACTIONS

The talks given and meetings attended by the P.I. during the reporting period are:

Yale; Seminar, April 5, 1989

UTRC; Seminar, April 6, 1989

MIT; Seminar, April 7, 1989

University of Michigan; AFOSR Contractors Meeting, June 19-21, 1989

Rocketdyne Div.; Consulting

Boeing Aerospace; Consulting

NASA Ames, APS/DFD Meeting; November 19-21, 1989

# TURBULENT MIXING IN ACCELERATING TRANSVERSE JETS

Adnan Eroglu\*

University of Washington, Seattle, WA 98195

## Abstract

The effects of acceleration on turbulent entrainment and structure of large scale vortices have been investigated in water tunnel experiments on the longitudinal vortex pair of an exponential jet in a cross-flow. The injection speed and the nozzle width of the jet both increased exponentially in the downstream direction of the cross-flow. An acceleration parameter  $\alpha$  is defined as the ratio of the revolution time of the longitudinal vortex pair to the e-folding time of the acceleration. It was found that the diameter of each vortex in the near-field jet cross-section is reduced more than a factor of three as  $\alpha$  is increased. In the same  $\alpha$  range, the jet flame length increased up to 50 %, revealing a strong effect of the near field forcing on the far field molecular scale mixing. Furthermore, the experiments have shown that the variation in size and strength of the counter-rotating vortex pair is not reflected upon the flame length variation for a certain range of jet to cross-flow velocity ratio. Thus, contrary to traditional modeling of the transverse jet entrainment in terms of a longitudinal vortex pair, a new three-dimensional description of the flow structure is given, in which entrainment of the cross-flow fluid into the jet relies heavily on the ring vortices which form a curved shear layer on the periphery of the jet.

## Nomenclature

$d_0$	nozzle width at $x = 0$
$d_j$	nozzle width at any $x$
$d_h$	hydraulic diameter
$R$	jet-to-free stream velocity ratio
$Re$	Reynolds number
$s$	center-to-center vortex spacing
$t$	time
$t_e$	e-folding time of the exponential acceleration function
$t_n$	nozzle time
$V_0$	jet velocity at $x = 0$
$V_j$	jet velocity at any $x$
$V_\infty$	uniform cross-flow speed

$x$	streamwise coordinate
$x_e$	e-folding distance of the exponential acceleration function
$x_f$	flame length
$\alpha$	acceleration parameter
$\delta$	vortex size
$\phi$	equivalence ratio

## Introduction

The purpose of this research is to explore the response of large scale vortices to externally applied acceleration. A recent theoretical notion suggests a significant change in the entrainment behavior of large scale vortices under suitable temporal or spatial accelerations,<sup>1,2</sup> e.g. an exponential acceleration function with an e-folding time comparable to the rotation period of the large scale vortices. According to this thinking, it would be possible to control the entrainment carried out by large scale vortices, provided that this acceleration requirement is satisfied.

The concept of utilizing an external acceleration or forcing to control large scale turbulent mixing is potentially applicable to numerous free shear flow problems. This study has mainly concentrated on controlling the interaction of a jet with a uniform cross-flow, with practical interest in mixing of a fuel jet with a transverse air stream. For a conventional jet, the injected fluid becomes progressively more dilute as it moves away from the nozzle, so all mixture ratios are eventually achieved. However, for applications such as combustion and chemical reaction processes, it is desirable to control the mixing, so that the reaction takes place at the optimum mixture ratio. Moreover, for a fuel jet introduced into a uniform cross-flow, isolating the injection process from mixing is desirable in order to provide better penetration of the fuel into the cross-stream, and to inhibit the combustion instabilities associated with the near field of the injection.

The earliest experimental work aimed at testing the validity of the concept mentioned above was conducted by Kato et al.<sup>3</sup> with a free round jet of constant diameter. Their results indicated about a 25 % increase in flame length over an equivalent steady jet when the injection speed increased linearly in time.

\*Graduate Research Assistant, Department of Aeronautics and Astronautics.

Copyright ©1990 by the American Institute of Aeronautics and Astronautics, Inc. All rights reserved.

More recent experiments<sup>4</sup> with a free jet have demonstrated a dramatic reduction in the growth rate of the jet, (about 36 % reduction in the spreading angle of the jet) when both the jet injection area and speed increase exponentially in time. However, no flame length data were available at the time of this writing to relate this observation to the mixing behavior of the jet. The experiments conducted by Clement and Rodriguez<sup>5</sup> in a supersonic tunnel with an array of discrete sonic jets of exponentially increasing diameter have demonstrated a much weaker bow shock ahead of the injection location compared to a single jet of equal momentum flux. Although they observed a nearly uniform jet fluid concentration in the near field of the injection, the supersonic flow conditions and the visualization technique they used did not allow a detailed analysis of the entrainment structure.

A turbulent jet in a cross-flow was studied here. However in this study, instead of a conventional transverse jet of uniform speed introduced through a circular orifice, both the jet injection width and injection speed were increased exponentially with downstream distance. The resulting flow was studied relying extensively on flow visualization techniques such as inert dye injection and laser induced fluorescence (LIF). Molecular scale mixing was analyzed by utilizing an acid-base reaction. Employing water for the fluid has proved to be an extremely powerful technique for a detailed analysis of the flow, yet a complete study aimed at a practical combustion problem should include the effects of heat release and compressibility.

### Round Steady Jet

Because of its numerous practical applications, ranging from combustion and thrust control to environmental disposal of effluents into the atmosphere and water bodies, the jet in a cross-flow has been studied for several decades.<sup>6-23</sup> Although a detailed description of this flow is still subject to debate, a commonly observed view of this flow can be given as illustrated in figure 1.

The prominent features of the flow field are that the jet fluid is deflected in the direction of the cross-flow as its cross-section quickly takes a kidney shape, dominated by a pair of counter-rotating vortices. A mixing layer develops on the periphery of the jet as the potential core of the jet ends as a cone, slightly bent in the direction of the cross-flow. Even though the existence of the shear layer ring vortices around the jet and the vortices formed in the wake of the jet have been observed experimentally, it has been explicitly stated<sup>11,13,14</sup> or implied in the literature that the entrainment into the jet is mainly due to the counter-rotating vortex pair, observed in the cross-section of

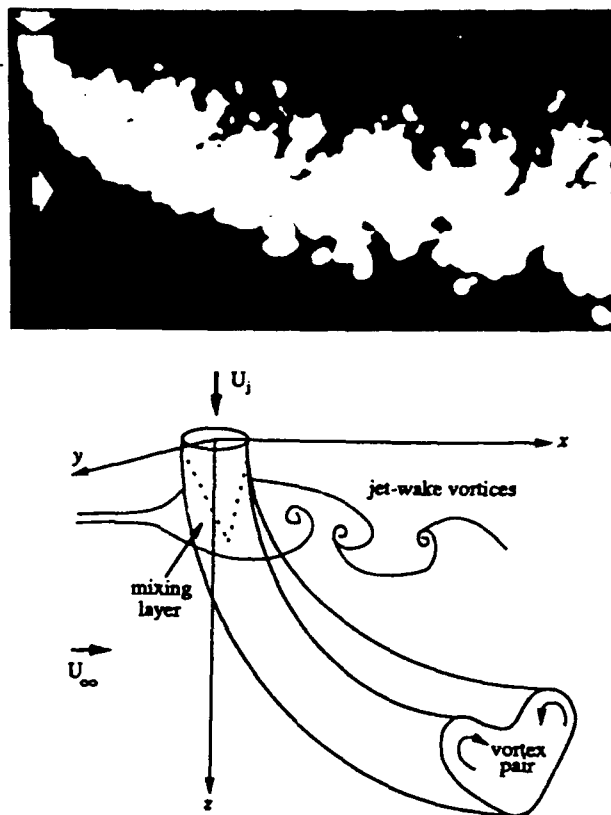


Figure 1: The round turbulent jet in a cross-flow

the jet. As a result, a significant portion of the earlier research has concentrated mainly on the structure of the jet cross-section, either measuring,<sup>6,11,13,21</sup> theoretically modeling,<sup>8,18,19</sup> or computing<sup>16,20,22</sup> the strength and spacing of the vortex pair.

Initially, this research was based on the assumption that the longitudinal vortex pair is the primary structure for large scale entrainment in a transverse jet. Consequently, an acceleration scheme was adapted to affect mainly this vortex pair by means of an acceleration function applied along the injection region. As the work has progressed, it was observed that the vortex pair responds to the acceleration by rapidly shrinking in size and the flame length of the jet increases. However, increasing the acceleration parameter above a certain value does not cause a significant change in the size of the vortices, but surprisingly the flame length of the jet drops gradually with increasing acceleration parameter. This behavior can not be explained on the basis of the counter-rotating vortex pair entrainment model. Because, as mentioned above, the size of the vortex pair stays about the same, and its strength decreases (as will be described later), suggesting less entrainment thus, a longer flame length. This leads one to conclude that

the entrainment structure is more complicated than the commonly utilized model of two-dimensional vortex sheet rolled-up to a pair of counter rotating vortices. An important contribution from the shear layer ring vortices formed around the jet is emphasized here to explain the (three-dimensional) structure of the flow.

### Vorticity Dynamics

During the last decade it has been demonstrated that large scale vortical structures can be forced externally such that the interaction among discrete vortices can be controlled in order to reduce or enhance mixing. Among the various flows related to this, the forced shear layer,<sup>26,27</sup> pulsed free jet,<sup>31</sup> and pulsed transverse jet<sup>32</sup> can be listed. In all of these experiments, it was observed that imposing an external time scale on the interaction process of large scale vortices changes the average flow properties such as the growth rate of a shear layer or a jet and the penetration depth of a transverse jet.

The goal of the experiments reported here can be related to the work listed above, namely altering the nonsteady interaction among the organized vortical structures by external forcing. Yet, the approach taken is significantly different and relies primarily on controlling the turn-over time and the strength of the vortices rather than their formation frequency, such that the interaction among these large scale structures can be dictated by external means.

The theory behind the exponential acceleration scheme<sup>1,2</sup> can be summarized as follows. For all unforced self-similar flows, global vorticity of each vortex decays inversely proportional to its own Lagrangian age. This can be verified on the grounds of dimensional analysis since the age of the vortex is the only time scale entering the problem. Physically, dilution of vorticity is mainly due to incorporation of the irrotational ambient fluid into the vortex. A vortex of size  $\delta$  (m) and circulation  $\Gamma$  ( $m^2/s$ ) has a volume engulfment appetite of order  $\delta\Gamma$ . In order to satisfy this appetite, a vortex formed at the near field injection region of a free jet, for example, engulfs both the ambient fluid, and the jet fluid injected at a later instant as it moves downstream.

It is proposed that imposing a new time scale on the flow would alter the aging characteristics of the vortices. Assume that the submerged jet fluid is accelerated as it exits from the nozzle with an acceleration function that has a time constant  $t_a$ . Then, it is plausible to expect a vortex to preferentially engulf the rotational jet fluid injected at a later time rather than the ambient fluid, since the acceleration would place the newly injected fluid at the back side of the vortex, the observed location of large scale

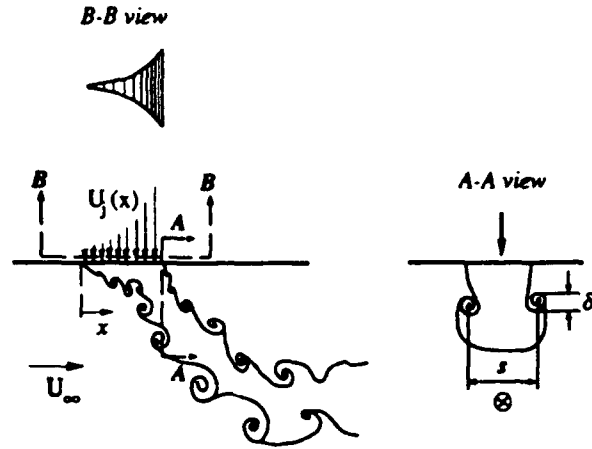


Figure 2: Exponential jet in a cross-flow, streamwise and transverse cross-sections.

entrainment.<sup>24,25</sup> Therefore, entrainment of the ambient fluid into each vortex would be limited by the externally applied acceleration conditions.

Entrainment by a vortex requires about a full vortex rotation.<sup>28,29</sup> This implies, for the case of the acceleration time constant being equal to the turn-over time of the vortices, that there would be little entrainment of the ambient fluid into the vortices since the engulfment appetite of each vortex is predominantly satisfied by the accelerating jet fluid. This corresponds to the case of little mixing of the jet fluid with the ambient fluid during the acceleration.

Implementation of this concept is carried out here by replacing the time coordinate with a spatial one. Namely, in these experiments the jet diameter and the injection speed do not vary in time but both increase exponentially with downstream distance. More specifically;

$$d_j(x) = d_0 e^{x/z_0} \quad (1)$$

$$V_j(x) = V_0 e^{x/z_0} \quad (2)$$

The spatial 'nonsteadiness' is brought into the problem by introducing this jet into a cross-flow as illustrated in figure 2. Then, as a cross-flow fluid element moves along the accelerating injection region, it feels an exponentially increasing impulse due to the jet fluid.

By using simple dimensional analysis techniques, the characteristic time scale associated with the revolution of each vortex in the vortex pair that is formed along the injection can be expressed as the ratio of the local injection width to the local injection speed,

$$t_n = \frac{d_j(x)}{V_j(x)} \quad (3)$$

which is termed the local nozzle time. From (1) and (2),

$$t_n = \frac{d_0}{V_0} \quad (4)$$

yields a constant  $t_n$  along the injection length.

Imposing an acceleration on the flow introduces a new time scale. Since the acceleration function is exponential, this characteristic time scale is the e-folding time of this function,  $t_e$ , which can be defined as

$$t_e = \frac{x_e}{V_\infty}. \quad (5)$$

The significance of  $t_e$  is that as a fluid element is convected along the injection length with a speed of approximately  $V_\infty$ , it observes an e-folding increase in the impulse on it from the jet during this time period.

An acceleration parameter can be defined as the ratio of these two time scales,

$$\begin{aligned} \alpha &= \frac{t_n}{t_e} \\ &= \frac{d_0 V_\infty}{x_e V_0}. \end{aligned} \quad (6)$$

Theoretically, one should expect a significant change in the structure of the vortex pair when  $\alpha \cong 1$ , because the vortex pair would make about one revolution by the time it experiences an e-fold increase in acceleration. In other words, the rotation time of the vortex pair would be matched with the convection time of it along a distance where a significant change in acceleration occurs. Using the same argument, if  $\alpha \ll 1$ , the vortex pair will make many revolutions by the time it experiences significant acceleration. If  $\alpha \gg 1$ , then the vortex pair will rotate slowly compared to the rate of acceleration. Hence, for these two cases the acceleration should not be expected to alter the entrainment ability of the vortex pair.

### Experimental Facility

The facilities used include a water tunnel, two exponential nozzle arrays, a pressurized fluid supply system, and a 5 Watt Argon-ion laser and optical components required for the LIF experiments.

#### Water Tunnel

The experiments were conducted in a horizontal type recirculating water tunnel facility with a test section 3 m long and 70 cm square cross section. Test section flow speed was varied from 0 to 70 cm/sec by changing the frequency input of a 22.4 KW ac-motor, driving a centrifugal pump. The freestream turbulence intensity in the test section was measured by

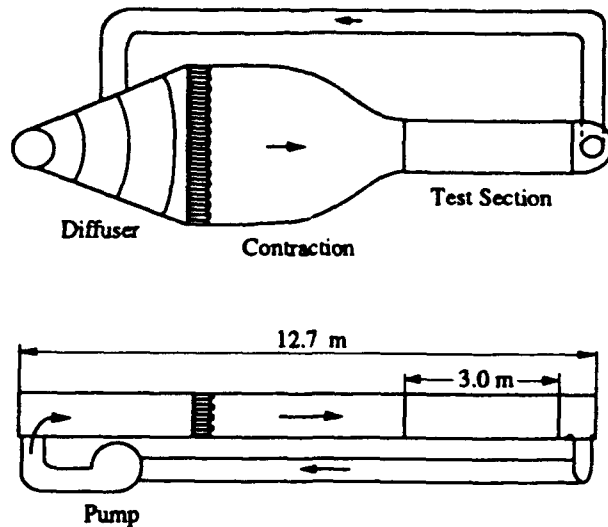


Figure 3: Water Tunnel Facility, top and side views.

using a hot film sensor operated at constant temperature mode and found to be less than 0.3 % of the mean flow speed. The water tunnel was constructed of stainless steel, tempered glass, and PVC pipes, therefore permitting the use of strong chemical solutions necessary for the flame length measurements. Vibrations caused by the pump and the flow inside the pipeline were isolated from the tunnel structure by using rubber coupling devices.

A simplified drawing of this facility is given in figure 3. A centrifugal pump is used to recirculate the fluid through a 28 cm diameter pipe that connects the test section exit to the diffuser inlet located at the opposite end of the tunnel. The flow enters the diffuser vertically, along a perforated tube with a tapered insert which reduces the tube's area linearly in order to distribute the flow at a uniform rate along the height of the tube. Three sets of perforated plates are installed along the 3.35 m long diffuser to prevent separation. A 3.05 m wide and 1.52 m long constant area settling chamber is located after the diffuser with a honeycomb-screen combination installed at 36 cm from its entrance. The honeycomb is built of 0.635 cm diameter plastic drinking straws, and a stainless steel wire screen with 0.0965 cm mesh size is installed at the exit plane of the honeycomb. A contraction section follows the settling chamber, with inlet to exit area ratio of four, and length of 3.81 m. The profile of the contraction is selected as a pair of matched cubic equations for the optimum reduction in the thickness of the boundary layers and turbulence intensity in the test section. The two side and bottom walls of the test section are made of single piece tempered glass



Nozzle Array A ( $d_0 = 0.6\text{cm}$ , $x_e = 8\text{cm}$ , $V_0 = 3\text{cm/sec}$ )					
$i$	$x_i$ cm	$x_{i+1}$ cm	$V_j$ cm/sec	$d_h$ cm	Re
1	0	3.7	3.8	1.26	482
2	3.75	6.2	5.6	1.57	880
3	6.25	8.8	7.8	1.94	1,513
4	8.85	11.3	10.7	2.28	2,441
5	11.35	13.8	14.6	2.62	3,839
6	13.85	16.3	20.0	2.98	5,975
7	16.35	18.85	27.4	3.38	9,258
8	18.9	21.4	37.7	3.66	13,823
9	21.45	22.7	47.6	2.16	10,302
10	22.75	24.0	56.0	2.18	12,234

Nozzle Array B-1 ( $d_0 = 0.3\text{cm}$ , $x_e = 3\text{cm}$ , $V_0 = 3\text{cm/sec}$ )					
$i$	$x_i$ cm	$x_{i+1}$ cm	$V_j$ cm/sec	$d_h$ cm	Re
1	0	2.4	4.8	0.73	356
2	2.45	4.85	10.9	1.33	1,457
3	4.9	6.15	19.3	1.41	2,729
4	6.2	7.5	30.2	1.65	5,000
5	7.55	8.8	46.8	1.78	8,358

Nozzle Array B-2 ( $d_0 = 0.3\text{cm}$ , $x_e = 3\text{cm}$ , $V_0 = 2\text{cm/sec}$ )					
$i$	$x_i$ cm	$x_{i+1}$ cm	$V_j$ cm/sec	$d_h$ cm	Re
1	0	2.4	3.2	0.73	236
2	2.45	4.85	7.3	1.33	969
3	4.9	6.15	12.9	1.41	1,819
4	6.2	7.5	20.1	1.65	3,318
5	7.55	8.8	31.2	1.78	5,552

Table 1: Flow parameters for the nozzle arrays.

panels for a full 3 m view from all directions. The top part of the test section is open.

### Nozzle Arrays

Two different nozzle arrays were used for the experiments reported here. The first nozzle array (referred to as A) includes 10 individual nozzles with a total injection length of 24 cm. The second array (referred to as B) is made of 5 nozzles with a total injection length of 9 cm. The e-folding distances are 8 cm and 3 cm for arrays A and B respectively, each array covering a total of three e-folding distances. Each nozzle in the B array consists of a combination of flow conditioning devices including foam, a perforated plate, a wire

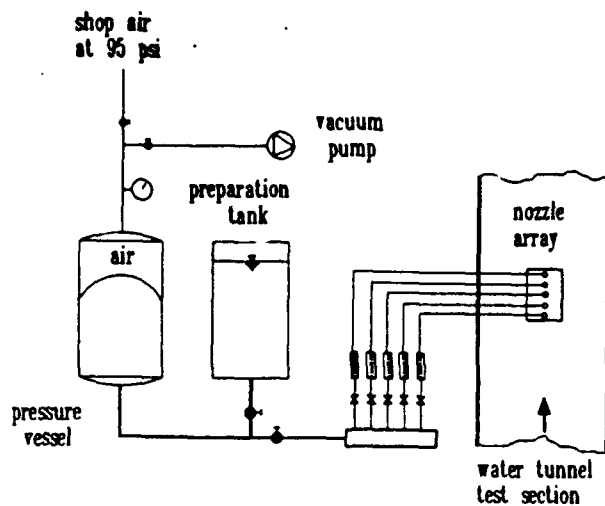


Figure 4: Fluid Supply System

screen, and a fifth order polynomial contraction. A simple linear contraction profile was used during the preliminary stages of the study carried out with the A array. Each individual nozzle was designed such that the array, built by stacking these nozzles together, would have a smooth, exponentially increasing injection width. Adjacent nozzles in each array were separated from each other by 0.05 cm thick stainless steel plates.

The speed increase of the injection was not continuous due to requirement of controlling the injection speed of each nozzle independently. The constant flow speed for each nozzle was calculated by dividing the integral of the exponential flow rate variation over the nozzle exit section by the nozzle exit area, i.e.

$$(V_j)_i = \frac{\int_{x_i}^{x_{i+1}} V_j(x) d_0 e^{x/x_e} dx}{\int_{x_i}^{x_{i+1}} d_0 e^{x/x_e} dx}$$

By increasing the number of nozzles in the arrays, an exponential injection speed increase was approached.

The nozzle array A was operated at one flow speed setting only, covering an acceleration parameter range of  $0.25 \leq \alpha \leq 1.6$ . The nozzle array B was tested at two different flow speed conditions referred to as B-1 and B-2, sweeping an acceleration parameter range of  $0.25 \leq \alpha \leq 2.0$  and  $0.25 \leq \alpha \leq 3.0$ , respectively. The acceleration parameter was varied by changing the cross-flow speed as the jet conditions were held constant at a specific setting.

The parameters describing the nozzle arrays and the individual nozzles included in each array are given in table 1. The lower limit of the acceleration parameter for each nozzle speed setting was chosen to minimize the effect of the bottom wall of the test section on the flow by restricting the jet penetration to a certain depth during the experiments. The maximum

speed of the water tunnel defined the upper limit of the acceleration parameter.

The exponential nozzle arrays were machined from clear Plexiglass and installed on a flat plate with elliptical leading edge and an adjustable flap at the trailing edge. This plate, installed 15 cm below the water free surface, acted as a false wall with adjustable boundary layer thickness.

### Fluid Supply System

A pressurized air driven system was used to supply each nozzle in the jet array with the constant volume flow rate necessary to make up the exponential transverse jet. Main components of this setup are shown in figure 2. The fluid to be injected is filled in the preparation tank from the tunnel in order to prevent any temperature difference and the resulting buoyancy effects between the primary and secondary flows. A vacuum pump was used to transfer the solution from the preparation tank to the pressure vessel by evacuating the air above a rubber diaphragm. During a run, driving pressure above the rubber diaphragm was held at 95 psi for all experiments. The exit of the pressure vessel was connected to a distribution manifold with ten outlets, each in turn connected to a precision regulating valve, a flow-meter, and one of the nozzles in the jet array.

### LIF System

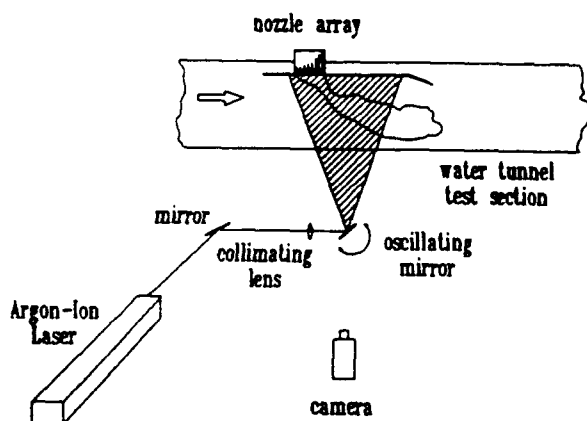


Figure 5: LIF Setup

A 5 Watt Argon-ion laser was used for illumination of the internal slices of the flow field using the LIF technique. The laser beam was passed through a collimating lens and reflected into the test section, as a sheet approximately 1 mm thick, by a mirror oscillating at 1200 Hz. LIF setup, illuminating a streamwise

cross-section of the flow, is shown in figure 5. Orientation of the illuminated plane was varied by re-arranging this basic setup, using additional mirrors. During the observation of transverse cross-sections of the jet, the optical components were mounted on a traversing mechanism to move the laser sheet in downstream direction in order to observe the structure of the counter-rotating vortex pair at different stations.

### Flow Visualization Techniques

The overall features of the jet plume as well as internal slices of the vortical structures were observed by using several techniques. The first technique used an inert dye in the jet fluid and visualizing the flow field by either diffuse background illumination or by spotlights positioned such that the interface can be best observed via shadow effects. It has proven to extremely powerful to use fluorescein dye for the inert dye experiments. Changing the dye concentration and the light intensity provided either a transparent or a fully opaque interface, clearly revealing both the internal interaction of the vortical structures and the outside shape.

The second technique illuminated internal slices of the jet using laser induced fluorescence (LIF) to excite a laser sensitive dye (sodium fluorescein) added to the jet fluid. Cross-sectional views of the jet perpendicular to the cross-flow direction were observed by using a submerged mirror, placed close to the downstream end of the test section to prevent disturbing the flow in the region studied.

The third method observed the transition of a pH indicator (phenolphthalein), triggered by an acid-base reaction between the jet and the cross-flow fluids. Sulfuric acid ( $H_2SO_4$ ) and sodium hydroxide (NaOH) water solutions were used in each stream. Upon mixing of the two streams at a prescribed volumetric ratio, the purple color of the pH indicator in the jet fluid was turned either on or off, revealing the location where the mixing at this ratio takes place. This ratio is referred to as the equivalence ratio  $\phi$ , and the visible length of the jet fluid is termed the flame length.

A 35 mm SLR camera was used for the pictures presented here. The vortex size and flame length measurements were made from the video recordings of the flow field. The camcorder recorded pictures at 30 frames per second with a shutter speed of 1/1000 of a second. The recordings taken with a zoom lens were further enlarged by a digital VCR on a large screen monitor up to 20 times of the original size, thus enhancing the accuracy of the measurements. A consistent method was used for measuring the fluctuating quantities throughout the experiments.

## Results and Discussion

### Vortex Structure



Figure 6: Streamwise internal cross-section of the exponential jet.

A streamwise cross-section of the exponential jet, observed at the symmetry plane is shown in figure 6. The mean penetration distance in the near-field of the injection increased exponentially along the injection region. After the injection was over, the jet fluid was quickly deflected in the cross-flow direction as in the case of a conventional transverse jet. The mean penetration distance normalized by the local injection width of the jet was found to be constant along the streamwise injection length of the jet, indicating a self-similar structure.

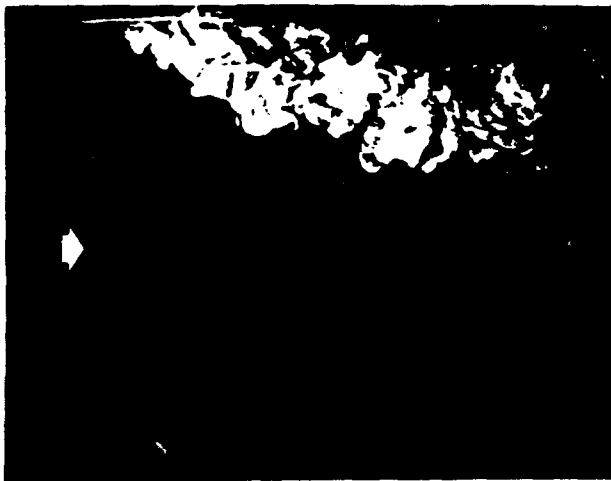


Figure 7: Streamwise outside view of the exponential jet.

A streamwise view of the exponential jet, illuminated by spotlights is given in figure 7. As can be

seen from this picture, a curved shear layer develops into discrete ring vortices around the jet fluid. One distinct feature of these ring vortices is that the sign of the vorticity undergoes a change at some point along the injection, the exact location depending on the jet to cross-flow velocity ratio. The vortex rings formed at the interface initially rotate in the counterclockwise direction for almost all jet to cross-flow velocity ratios, because the early part of the jet is much slower than the cross-flow. However, as the jet speed increases downstream, the newly formed vortices rotate in the clockwise direction. The transition from one sign of vorticity to the other occurs in the form of a pairing, which takes place in an alternating manner. In other words, if the upstream vortex ring (rotating counterclockwise) comes into interaction with the downstream one (rotating clockwise) from the left side of it (as sketched in figure 2), the pair rapidly propagates upward, as a result of their self-induced velocity. On the other hand if the pairing takes place on the right side of the clockwise rotating downstream vortex ring, then the pair propagates downward into the cross-flow. In both cases the weaker vortex is ultimately incorporated in the stronger one as they move downstream, forming a single vortex rotating in the clockwise direction.

The size of the shear layer ring vortices increases in the downstream direction as they entrain the cross-flow fluid. However, partly due to the sign change mentioned above, and primarily due to the continuous decline in the radius of curvature of the jet penetration profile, their growth rate was found to be suppressed along the injection length compared to a conventional single jet in a cross-flow.

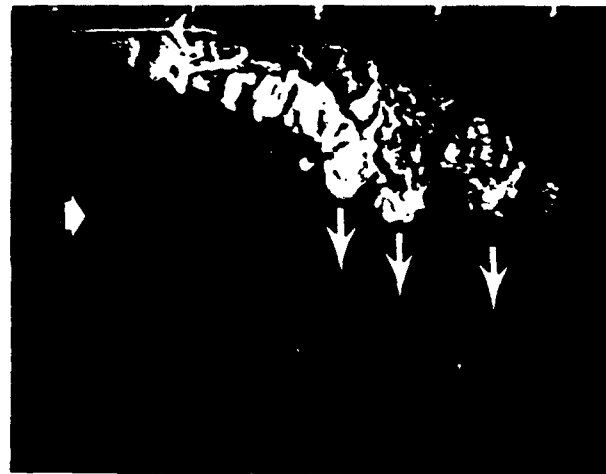


Figure 8: Periodic bursts into the crossflow as a result of vortex pairing.

The most interesting feature of the flow structure was observed in the region immediately after the in-



Figure 9: Large scale structures in the far-field of the exponential jet

jection length. As indicated above, the jet penetration profile is quickly deflected in the direction of the cross-flow after the injection is over. Although there is still a debate in the literature on the exact mechanism that causes the jet to deflect, the observed structure for an accelerating jet indicates that the shear layer ring vortices quickly grow in this region to erode the unmixed jet core. The intriguing feature of these ring vortices can be described as follows. Under the shear forces imposed on them by the existence of the cross-flow, they undergo a circumferential stretching, directed towards the lee side of the jet. Then, the portion of the ring stretched into the lee side is deflected upstream along the jet center line and tilted downward towards the windward side of the jet. That is to say, after the injection region, the shear layer ring vortices are subject to both circumferential stretching and longitudinal distortion. A similar behavior of the vortex rings was predicted in the numerical study of Sykes et al.<sup>20</sup> for a round transverse jet. Naturally, this deflection causes the portion of ring vortices deflected as stated above to come into contact with the neighboring upstream ring vortices. The result is a pair of curved line vortices of opposite sign, laterally penetrating into the cross-flow from the windward side of the jet. This is a repeated phenomenon, causing periodic "bursts" into the cross-flow as shown in figure 8. Consequently, as pointed at in figures 6 and 9, the jet structure in the far field is not continuous, but instead consists of these distorted ring vortices undergoing a periodic pairing process.

In addition to the distortion and the resulting pairing of the vortex rings discussed above, another distortion mechanism was observed as shown in figure 10. This is similar to the Widnall instability, observed as the growth of waves around a vortex ring. The lo-



Figure 10: Instability of an individual vortex ring.

cation where these waves first can be seen varies, depending on jet Reynolds number and jet to cross-flow velocity ratio.



Figure 11: Transverse cross-section of the exponential jet

If the laser sheet is placed perpendicular to cross-flow direction at some point along the injection region, a cross-section of the jet is visualized as shown in figure 11. A pair of counter-rotating vortices, giving a mushroom shape to this cross-section can be observed. As the main emphasis was placed on studying the response of this vortex pair to acceleration, a significant effort was made to measure their size and spacing as a function of acceleration parameter  $\alpha$ . It was observed that although the jet cross-section maintains its mushroom shape, its size fluctuates in time as the ring vortices formed around the jet pass through the observation plane at a certain frequency. And since these ring vortices extend to envelope the

longitudinal vortex pair, their passage causes the size of this vortex pair to fluctuate in time also. A consistent averaging technique was employed for the results reported here.

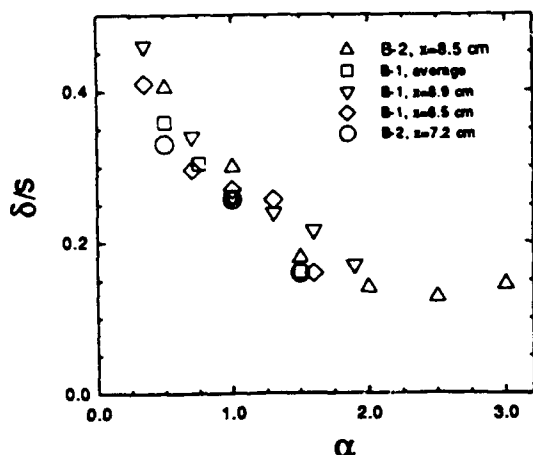


Figure 12: Normalized vortex size variation with  $\alpha$

The size and spacing of the counter-rotating vortex pair were measured within the acceleration parameter range of  $0.25 \leq \alpha \leq 3.0$ . The variation in the size of these vortices, normalized by their center to center spacing, with acceleration parameter is given in figure 12. A similar behavior was observed for all nozzle arrays tested. That is, the vortices first declined in size as  $\alpha$  is increased. But  $\delta/s$  reached an asymptotic value at approximately  $\alpha = 2$ , and no significant change in the size of the vortices was observed beyond this point. However, in this range of  $\alpha$ , the roll-up process for the initial formation of the vortex pair itself was intermittent. Namely, the fluctuations in the size of the vortices, observed in the lower  $\alpha$  region, were replaced by periodic disappearance of the full structure.

#### Flame Length and Mixing

The mixing structure observed by using an acid-base reaction coupled with the LIF technique reveals that the first place where the jet fluid mixes fully with the cross-flow for a given equivalence ratio is located on the lee side of the jet. The last place where the unmixed jet fluid can be observed is always at the windward side of the jet. Furthermore, the visible location of the flame tip undergoes periodic fluctuations, and fluctuation length increases with increasing total flame length. This is analogous to the fluctuations observed in the flame length of a free jet or thermal, associated with the large scale structure.<sup>24,25</sup>

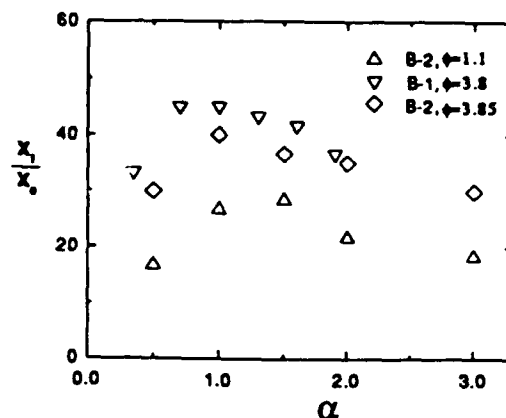


Figure 13: Flame length variation of the exponential jet with  $\alpha$

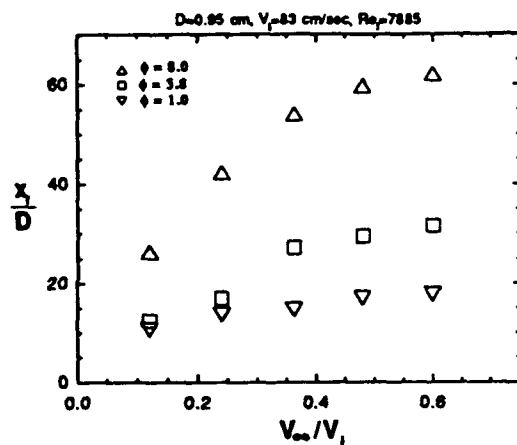


Figure 14: Flame length variation for a round jet in a cross-flow

The flame length of the exponential jets B-1 and B-2 were measured at two different equivalence ratios; the results are given in figure 13. A significant increase is observed in the flame length as  $\alpha$  nears unity. However, increasing  $\alpha$  after this point causes the flame length to decrease back to nearly its unforced value.

The flame length of a round steady jet was measured and results are given in figure 14. The flame length data for the exponential jet, given in figure 13, correspond to the region in figure 14 where  $V_\infty/V_j$  is greater than 0.5. The data from figure 14 suggest that, for a conventional jet there is essentially no change in the flame length (especially for  $\phi = 1.0$ ) above  $V_\infty/V_j = 0.4$ . Whereas, for the exponential jet,

the flame length increases about 50 % in this velocity ratio range.

The first part of the curve in figure 13, the increase in the flame length, can be attributed to the decrease in the size of the vortex pair observed for the same  $\alpha$  range. On the other hand, the region where the flame length decreases even as the vortex pair stays the same size is ambiguous. According to experimental data by Fearn and Weston,<sup>11</sup> the strength of the vortex pair decreases as the jet to cross-flow velocity ratio  $R$  decreases. Consequently, since  $\alpha \sim 1/R$ , increasing  $\alpha$  means weaker vortices, thus less mixing. Whereas, the opposite is observed from figure 13, i.e., the flame length decreases with increasing  $\alpha$ , indicating more mixing.

Two factors can be listed as a possible explanation. The first one is that, although the visible size of the vortex pair does not change after  $\alpha \simeq 2.0$ , the ability of the pair to incorporate the jet fluid along the injection could decrease as it is convected below the injection region too fast, so that it would not make enough revolutions in the injection region. Thus it is plausible to expect the jet to mix with the cross-flow faster as  $\alpha$  is increased beyond unity. The second factor has to do with the shear layer ring vortices formed around the jet. The flow visualization experiments have demonstrated that the shear layer ring vortices are in fact capable of entraining and consuming a significant portion of the cross-flow fluid mixing with the jet. They form early in the injection region and exist far downstream, dominating the flow structure. Thus, this unexpected flame length behavior may be attributed to the entrainment carried out by the shear layer ring vortices, and may suggest that the jet in cross-flow needs to be further studied by concentrating on the shear layer ring vortices.

### Conclusions

Imposing an external time scale on large scale structure of a jet in a cross-flow alters its entrainment and mixing characteristics significantly. This, in practice, can provide one with a valuable tool, other than jet to cross-flow momentum ratio, to control mixing and penetration of a jet in a cross-flow. Even though the concept of the accelerating transverse jet is new and requires further testing, the experiments reported here have shown that it may find important use in combustion and chemical processes where entrainment and mixing have significant effects on overall processes.

On the other hand, it was also observed that, because of a three-dimensional effects, modeling of a jet in a cross-flow only in terms of a pair of counter-rotating vortices does not represent the actual entrainment mechanism. The significant contribution

from the shear layer ring vortices and a distortion and pairing process imposed on them by the existence of the counter-rotating vortex pair has to be included in a complete study of this flow.

### Acknowledgements

The author wishes to express his appreciation to Professor Robert E. Breidenthal for his guidance and support throughout this study. This project was supported by the Air Force Office of Scientific Research under Grant No. AFOSR-87-0366, whose support is gratefully acknowledged.

### References

- [1] Breidenthal, R.E., "Turbulent Mixing in Accelerating Jets", Proceedings of the IUTAM Symposium, Bangalore, India, Springer-Verlag, New York, 1987.
- [2] Breidenthal, R., "The turbulent exponential jet", *Phys. Fluids*, 29, 1986, pp. 2346-2347.
- [3] Kato, S.M., Groenwegen, B.C., and Breidenthal, R.E., "On turbulent mixing in nonsteady jets", *AIAA Journal*, Jan. 1987, pp. 165-168 and Breidenthal et al., *AIAA Paper 86-0042*, Reno, Nevada, 1987.
- [4] Li, H., private communication.
- [5] Clement, P. and Rodriguez, C., "Shock Wave Structure and Penetration Height in Transverse Jets", *AIAA Student Journal*, Vol. 27, No. 2, Summer 1989, pp. 7-16.
- [6] Keffer, J.F. and Baines, W.D., "The round turbulent jet in a cross-wind", *J. Fluid Mech.*, Vol. 14, No. 4, 1963, pp. 481-496.
- [7] Pratte, B.D. and Baines, W.D., "Profiles of the Round Turbulent Jet in a Cross Flow", *J. Hyd. Div., Proc. ASCE*, HY6, Vol. 93, 1967, pp. 53-64; corrections, HY3, Vol. 94, May 1968, pp. 815-816.
- [8] Durando, N.A., "Vortices Induced in a Jet by a Subsonic Cross Flow", *AIAA Journal*, Vol. 9, 1971, pp. 325-327.
- [9] Kamatoni, Y. and Greber, I., "Experiments on a Turbulent Jet in a Cross Flow", *AIAA Journal*, Vol. 10, No. 11, Nov. 1972, pp. 1425-1429.
- [10] McMahon, H.M., Hester, D.D., and Palfrey, J.G., "Vortex Shedding from a Turbulent Jet in a Cross-Wind", *J. Fluid Mech.*, Vol. 48, 1971, pp. 73-80.

- [11] Fearn, R. and Weston, R.P., "Vorticity Associated with a Jet in a Cross Flow", *AIAA Journal*, Vol. 12, No. 12, Dec. 1974, pp. 1666-1671.
- [12] Chassaing, P., George, J., Claria, A., and Sananes, F., "Physical Characteristics of Subsonic Jets in a Cross-Stream", *J. Fluid Mech.*, Vol. 62, 1974, pp. 41-64.
- [13] Moussa, Z.M., Trischka, J.W., and Eskinazi, S., "The Near Field in the Mixing of a Round Jet with a Cross-Stream", *J. Fluid Mech.*, Vol. 80, 1977, pp. 49-80.
- [14] Le Grivés, E., "Mixing Process Induced by the Vorticity Associated with the Penetration of a Jet into a Cross Flow", *J. of Engineering for Power*, Vol. 100, July 1978, pp. 465-475.
- [15] Rathgeber, D.E. and Becker, H.A., "Mixing Between a Round Jet and a Transverse Turbulent Pipe Flow", *The Canadian Journal of Chemical Engineering*, Vol. 61, April 1983, pp. 148-157.
- [16] Patankar, S.V., Basu, D.K., and Alpay, S.A., "Prediction of the Three-Dimensional Velocity Field of a Deflected Turbulent Jet", *ASME, J. of Fluids Eng.*, Dec. 1977, pp. 758-762.
- [17] Andreopoulos, J. and Rodi, W., "Experimental Investigation of Jets in a Crossflow", *J. Fluid Mech.*, Vol. 138, 1984, pp. 93-127.
- [18] Broadwell, J.E. and Breidenthal, R.E., "Structure and Mixing of a Transverse Jet in Incompressible Flow", *J. Fluid Mech.*, Vol. 148, 1984, pp. 405-412.
- [19] Karagozian, A.R. and Greber, I., "An Analytical Model for the Vorticity Associated with a Transverse Jet", *AIAA 17th Fluid Dyn., Plasma Dyn. & Las. Conf.*, 1984.
- [20] Sykes, R.I., Lewellen, W.S., and Parker, S.F., "On the vorticity dynamics of a turbulent jet in a crossflow", *J. Fluid Mech.*, Vol. 168, 1986, pp. 393-413.
- [21] Savory, E., Toy, N., and Hossain, N., "An Experimental Study of the Potential Flow Parameters Associated with a Jet in a Crossflow", *AIAA/ASME/SIAM/APS First National Fluid Dynamics Congress*, July 25-28, Cincinnati, Ohio, A Collection of Technical Papers, Part 2.
- [22] Coelho, S.L.V. and Hunt, J.C.R., "The Dynamics of the Near Field of Strong Jets in Crossflows", *J. Fluid Mech.*, Vol. 200, 1989, pp. 95-120.
- [23] Fric, T.F. and Roshko, A., "Structure in the Near Field of the Transverse Jet", Presented at the 7th Symposium on Turbulent Shear Flows at Stanford University, August 21-23, 1989.
- [24] Johari, H., "An Experimental Investigation of Mixing in Buoyant Flows", Ph.D. thesis, University of Washington, 1989.
- [25] Dahm, W.J.A., "Experiments on entrainment, mixing and chemical reactions in turbulent jets at high Schmidt number", Ph.D. thesis, California Institute of Technology, 1985.
- [26] Oster, D. and Wygnanski, I., "The forced mixing layer between parallel streams", *J. Fluid Mech.*, Vol. 123, 1982, pp. 91-130.
- [27] Roberts, F.A., "Effects of a periodic disturbance on structure and mixing in turbulent shear flows and wakes", Ph.D. thesis, California Institute of Technology, 1985.
- [28] Dimotakis, P.E. and Brown, G.L., "The mixing layer at high Reynolds number: large structure dynamics and entrainment", *J. Fluid Mech.*, Vol. 78, 1976, pp. 535-560.
- [29] Broadwell, J.E. and Breidenthal, R.E., "A simple model of mixing and chemical reaction in a turbulent shear layer", *J. Fluid Mech.*, Vol. 125, 1982, pp. 397-410.
- [30] Gollahalli, S.R., Brzustowski, T.A., and Sullivan, H.F., "Characteristics of a Turbulent Propane Diffusion Flame in a Cross-Wind", *Transactions of the CSME*, Vol. 3, No. 4, 1975, pp. 205-214.
- [31] Koch, C.R., Mungal, M.G., Reynolds, W.C., and Powell, J.D., "Helical Modes in Acoustically Excited Round Air Jet", *Phys. Fluids A*, Vol. 1, No. 9, September 1989.
- [32] Wu, J.M., Vakili, A.D., and Yu, F.M., "Investigation of the Interacting Flow of Nonsymmetric Jets in Crossflow", *AIAA Journal*, Vol. 26, No. 8, Aug. 1988.